International Journal of Pharmaceutics 420 (2011) 274–281

Contents lists available at SciVerse ScienceDirect

International Journal of Pharmaceutics

journal homepage: www.elsevier.com/locate/ijpharm

In-line monitoring and interpretation of an indomethacin anti-solvent crystallization process by near-infrared spectroscopy (NIRS)

Hea-Eun Lee[a], Min-Jeong Lee[b], Woo-Sik Kim[c], Myung-Yung Jeong[d], Young-Sang Cho[e], Guang Jin Choi[a,b,*]

[a] Department of Pharmaceutical Engg., Inje University, Gimhae, Gyeungnam 621-749, Republic of Korea
[b] Department of Smart Foods and Drugs, Inje University, Gimhae, Gyeungnam 621-749, Republic of Korea
[c] Department of Chem. Engg., ILRI, Kyung Hee University, Yongin, Gyeonggi 446-701, Republic of Korea
[d] WCU Department of Cogno-Mechatronics Engg., Pusan Nat. Univ., Busan 609-735, Republic of Korea
[e] Energy Division, Korea Institute of Science & Technology, Seoul 136-791, Republic of Korea

ARTICLE INFO

Article history:
Received 24 May 2011
Received in revised form 19 August 2011
Accepted 29 August 2011
Available online 2 September 2011

Keywords:
Indomethacin (IMC)
Polymorphism
Anti-solvent crystallization
Near-infrared spectroscopy (NIRS)
Principal component analysis (PCA)

ABSTRACT

PAT (process analytical technology) has been emphasized as one of key elements for the full implementation of QbD (quality-by-design) in the pharmaceutical area. NIRS (near-infrared spectroscopy) has been studied intensively as an in-line/on-line monitoring tool in chemical and biomedical industries. A precise and reliable monitoring of the particle characteristics during crystallization along with a suitable control strategy should be highly encouraged for the conformance to new quality system of pharmaceutical products. In this study, the anti-solvent crystallization process of indomethacin (IMC) was monitored using an in-line NIRS. IMC powders were produced via anti-solvent crystallization using two schemes; 'S-to-A' (solvent-to-antisolvent) and 'A-to-S' (antisolvent-to-solvent). In-line NIR spectra were analyzed by a PCA (principal component analysis) method. Although pure α-form IMC powder was resulted under A-to-S scheme, a mixture of the α-form and γ-form was produced for S-to-A case. By integrating the PCA results with off-line characterization (SEM, XRD, DSC) data, the crystallization process under each scheme was elucidated by three distinct consecutive steps. It was demonstrated that in-line NIRS, combined with PCA, can be very useful to monitor in real time and interpret the anti-solvent crystallization process with respect to the polymorphism and particle size.

1. Introduction

Most active pharmaceutical ingredient (API) powders may exist in more than one crystalline form, which is known as, polymorphism. Polymorphs are defined as different arrangements or conformations of the molecules within the crystal lattice (Masuda et al., 2006). It is well known that the physicochemical properties of APIs, such as solubility, stability, and processability, are strongly dependent upon the class of polymorph. In this context, the polymorphic purity of APIs must be controlled and assured during the crystallization process.

Indomethacin (IMC; [1-(4-chlorobenzoyl)-5-methoxy-2-methyl-1*H*-indole-3-yl] acetic acid) has been used in many pharmaceutical preparations as an anti-inflammatory and anti-pyretic drug (Winter et al., 1963; Chieng et al., 2009). IMC has been reported to present a complicated polymorphism showing five true polymorphs, thus far, and a wide range of solvate forms (Slavin et al., 2002). Among them, only two, referred to as the γ-form (I) and the α-form (II), are regularly produced and are potentially the most useful forms. The γ-form is the most thermodynamically stable as implied by the melting point. Although meta-stable, the α-form can be prepared by direct crystallization and has been shown to persist at room temperature for periods of longer than 18 months without transformation. The γ-form shows a well-defined morphology with a plate-like structure, whereas the α-form grows as a fibrous or spherulitic structure (Slavin et al., 2002). A thermodynamically calculated value of the transition temperature between the γ-form and the α-form was unrealistically high at 534 °C (Urakami et al., 2002). Accordingly, the IMC polymorphism between the γ-form and the α-form was regarded as a monotropic system.

There have been reports on the relationship between the IMC polymorphs and the biological absorption rate (Yokoyama et al., 1979; Masuda et al., 2006). In general, since the dissolution rate of the meta-stable form is more rapid than that of the stable form, the biological absorption rate of the meta-stable form is also greater than that of the stable form. For IMC, it has been reported that

* Corresponding author at: Department of Pharmaceutical Engg., Inje University, Gimhae, Gyeungnam 621-749, Republic of Korea. Tel.: +82 55 320 3723; fax: +82 55 327 4955.
E-mail address: pegchoi@inje.ac.kr (G.J. Choi).

0378-5173/$ – see front matter © 2011 Elsevier B.V. All rights reserved.
doi:10.1016/j.ijpharm.2011.08.044

the rectal absorption rate of the meta-stable α-form in the rat was greater than the stable γ-form (Yokoyama et al., 1979).

Methods to produce various IMC polymorphs are well reviewed (Slavin et al., 2002). The α-form IMC is reportedly prepared by recrystallization and anti-solvent crystallization. Via recrystallization, IMC dissolved in ethanol at 70 °C was rapidly cooled to 4 °C, followed by filtration and vacuum drying at 40 °C (Masuda et al., 2006). Nonetheless, a pure α-form is rarely obtainable by the cooling approach (Takiyama et al., 2010).

It was reported that the pure α-form could be prepared by an anti-solvent method where an IMC-acetone solution was fed into water under vigorous agitation (Takiyama et al., 2010). On the other hand, when ethanol was used as the solvent, the α-form IMC was obtained by adding distilled water into the IMC solution at 80 °C (Kaneniwa et al., 1985). Precipitated crystals were removed by filtration and then dried under vacuum at 36 °C. According to our preliminary work, we attempted to obtain a pure α-form IMC powder by adding the IMC solution (in acetone) into the anti-solvent (water). Instead, the desired result was achieved by reversing the direction of addition.

The anti-solvent approach for crystallization has been known as a powerful isolation and purification technique, particularly when the temperature coefficient of solubility is low or the solute is not stable at elevated temperatures (O'Grady et al., 2007). Pronounced problems associated with it, however, include the batch-to-batch variability, poor uniformity in the shape of the resulting crystals, and solvate/hydrate formation. The effects of various critical process parameters have been investigated, such as the anti-solvent type (Takiyama et al., 1998; Oosterhof et al., 1999), solute concentration (Kaneko et al., 2002; Kitamura and Sugimoto, 2003), anti-solvent addition rate (Beckmann, 1999; Holmback and Rasmuson, 1999) and agitation intensity (Takiyama et al., 1998; Yu et al., 2005).

A strong trend has been set for research activities in the pharmaceutical industry and academia that are associated with in-line or on-line monitoring of critical quality attributes during pharmaceutical manufacturing processes, since two regulatory reports were issued by the US FDA. There two reports were titled, "Pharmaceutical CGMPs for the 21st century" (US-DHHS and US-FDA, 2002) and "PAT (process analytical technology) – a framework for innovative pharmaceutical development, manufacturing, and quality assurance" (US-DHHS and US-FDA, 2004).

There are not many study reports found in the literature regarding in-line/on-line measurements of IMC crystallization processes. X-ray crystallographic analysis has been performed to determine the crystal structures of IMC for the γ-form (Kistenmacher and Marsh, 1972) and for the α-form (Chen et al., 2002). Raman and NIR spectroscopy were used in combination to quantify the ternary mixture of IMC polymorphs (Heinz et al., 2007). A quantitative model was created, employing a PLS regression method. Polymorphic compositions of IMC in powders and tablets were measured by near-infrared spectroscopy (NIRS) (Otsuka et al., 2003). In this study, XRD peaks at $2\theta = 11.6^\circ$, 19.6°, 21.8°, and 26.6° were selected to estimate the γ-form content. However, these studies dealt only with IMC powders with a stationary state, not with an on-going process. In addition, FBRM was employed to detect the onset of nucleation for the anti-solvent crystallization process (O'Grady et al., 2007).

When it is desired to manufacture IMC powder of a high quality via anti-solvent crystallization process, it would be necessary not only to monitor transitions between polymorphs, but also to quantify the amount of crystalline and amorphous materials during the process. In this study, it was attempted for the first time to monitor and interpret the IMC anti-solvent crystallization process by in-line NIR measurements. Off-line characterization results were combined with PCA data to comprehensively understand the whole process of nucleation, crystal growth and polymorphic transition in three distinct steps.

2. Materials and methods

2.1. Materials

The γ-form of indomethacin (IMC) was purchased from Tokyo Chemical Industry (Tokyo, Japan). All solvents used in this study including acetone (Junsei Chemical Co., Japan), were of reagent grade or the best grade available. Water was purified employing a reverse-osmosis system (Nexpure, Korea) prior to use as an anti-solvent for IMC.

2.2. Reference standard samples

There are three reference standard samples, the γ-form, α-form and amorphous form. The commercial IMC powder was used as the γ-form standard, whereas the α-form standard was prepared by cooling crystallization in accordance with a previous report (Masuda et al., 2006). Two grams of the γ-form powder was dissolved in 7 mL of ethanol at 70 °C. Then, the solution was rapidly cooled to 4 °C and stored at this temperature overnight. The precipitated powders were collected by filtration using an aspirating glass funnel, followed by a vacuum drying at 40 °C. The amorphous powder was prepared by melting commercial IMC powder at 170 °C and by a rapid cooling at 4 °C.

2.3. Anti-solvent crystallization

The crystallization was carried out by mixing two liquids (an IMC-acetone solution and anti-solvent water) under two different schemes: (1) by adding instantaneously the whole IMC-acetone solution (~108 mL) into 500 mL water (referred to as 'S-to-A' scheme) and (2) by adding quickly 500 mL water into the IMC-acetone solution (referred to as 'A-to-S' scheme). This specific ratio was chosen by referring to a previous case study (Yokoyama et al., 1979). The IMC-acetone solution was prepared by dissolving 15 g of the γ-form IMC in 100 mL acetone at 54 °C, which approximately corresponds to a half of its solubility in acetone at 54 °C. As expected, these two schemes have brought about substantially contrasting results.

For both schemes, the crystallization flask was stirred at 300 rpm using an agitator (Wisestir™, HT-50D, DAIHAN Sci., Korea). The temperature was maintained at 54 °C throughout in an oil bath using a suitable PID controller. The whole solution after completion and/or 30 mL aliquots of the solution sampled at designated time points were filtered as quickly as possible using a vacuum-driven glass funnel installed with a 2.5 μm filter paper, followed by drying overnight under vacuum at 40 °C.

2.4. Near-infrared (NIR) spectroscopy and principal component analysis (PCA)

The experimental set-up of an anti-solvent crystallization apparatus connected with the fiber-optic NIRS is shown in Fig. 1. The NIR spectrometer (FTPA 2000-260; ABB Bomem, Quebec, Canada) was equipped with a tungsten-halogen source and an InGaAs diode array detector. A diffusive reflectance probe (FOCON FO; ABB Bomem) was integrated into the spectrophotometer using a 3-m long fiber-optic cable. NIR spectra were continuously collected in the wave-number range from 4000 to 14,000 cm^{-1} at a resolution of 64 cm^{-1}. Each spectrum was recorded by averaging 32 data scans, which took approximately 4 s. Since the total time of the whole crystallization process was 10 min, each process was represented

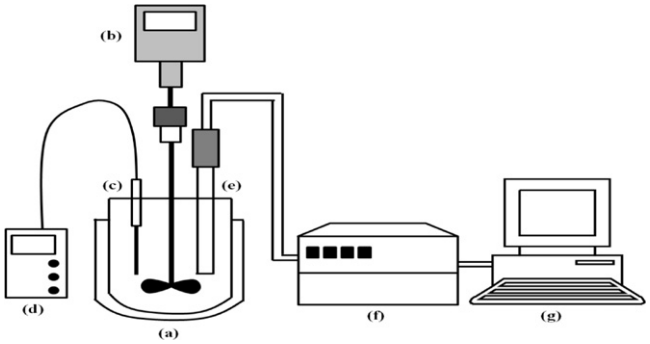

Fig. 1. A schematic diagram of experimental apparatus: (a) glass jacketed reactor, (b) agitator, (c) temperature probe, (d) temperature indicator, (e) NIR fiber-optics probe, (f) NIR main body and (g) personal computer.

with 150 NIR spectra. All measurements were carried out in triplicate to verify the reproducibility. For off-line characterization of in-process materials, solution samples were collected at designated time points such as 0.5, 1, 1.5, 2, 3, 5, 7 and 10 min.

All NIR spectra acquired from the in-line monitoring of anti-solvent crystallization processes were treated and analyzed using the GRAMS/AI 7.00 computer software (Galactic Ind., Salem, NH). Principal component analysis (PCA) was performed employing the PLS plus/IQ program in the GRAMS/AI 7.00.

2.5. Off-line characterizations

Scanning electron microscopy (SEM; Hitachi SE4300-SE, Japan) was employed to examine the morphology and size of IMC particles formed during the anti-solvent crystallization process. Every powder specimen was coated with gold by sputtering to avoid charging problems. The size estimated by SEM was confirmed by optical microscopy (Optika microscopes, Italy). The size estimation was performed for the representative area of 13.5 cm × 10 cm for each micrograph.

The crystalline structure of IMC powders was determined using a powder X-ray diffractometer (XRD; Rigaku MiniFlex$^+$, Japan) with Cu K_α radiation (λ = 1.54 Å @ 30 kV/15 mA). The XRD pattern for each powder sample was acquired at Bragg angle (2θ) of 5–20° with a scan speed of 0.5° per second. Two aspects of the XRD patterns were taken into account; the position and the peak area of major diffraction peaks. The former was used for polymorph identification while the latter was used for the approximate estimation of polymorphic fractions including the amorphous phase.

Pure γ-form and α-form IMC powders were compounded and measured in seven compositions (10, 20, 30, 50, 70, 80, and 90%) with amorphous diluents for XRD calibration. Each reference sample was blended in a mortar using a pestle for improved homogeneity. Two standard regression curves were created based on these reference calibrations, which both demonstrated fairly good correlations with R^2 values of 0.975 and 0.980 for the γ-form and the α-form, respectively (plots not shown). When polymorphic fractions were calculated, the quantity of powder sample was considered as well. The quantities of the γ-form and the α-form IMC were calculated from the peak areas of two representative peaks of Bragg angle 12.2–12.9° and 7.6–8.9°, respectively. As shown in Fig. 2, there is no appreciable superimposition between these two peaks. As a matter of fact, the 13.3–14.9° peak region was considered for the α-form quantification as well. These two results, however, were in a good agreement.

A differential scanning calorimetry (DSC) analyzer (Perkin Elmer Pyris 1, USA) was employed for the thermal analysis of the γ-form, α-form, and amorphous powders, primarily to confirm the XRD analysis results. In brief, 6 mg of each powder sample was placed onto a standard platinum pan and sealed. An empty pan was used as a reference. All DSC measurements were performed at a heating rate of 10 °C/min over the temperature range from 20 to 180 °C under a pure nitrogen atmosphere.

3. Results and discussion

Typical SEM micrographs and powder XRD patterns of standard IMC powders are illustrated in Fig. 2. Firstly, the γ-form shows a rather bulky morphology of a plate-like habit. On the other hand, the α-form has a definite needlelike shape. XRD patterns of the γ-form, α-form, amorphous form powders are compared in Fig. 2b. XRD peak positions of both standard powders were confirmed by those reported in the literature (Otsuka et al., 2003). The amorphous form showed a typical 'halo' XRD pattern. Although there was a substantial difference in the absolute peak intensity between the γ-form and α-form, our quantitative XRD analysis was readily performed due to the distinctive peak positions.

3.1. NIR spectra and PCA results

All NIR spectra were acquired in the wave-number range from 4000 to 14,000 cm^{-1} to monitor physicochemical changes

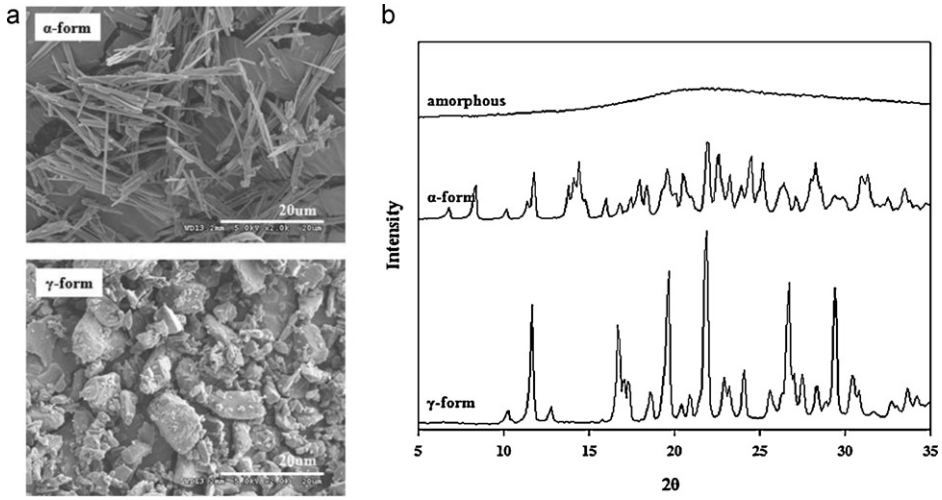

Fig. 2. SEM photographs and XRD patterns of standard IMC powders.

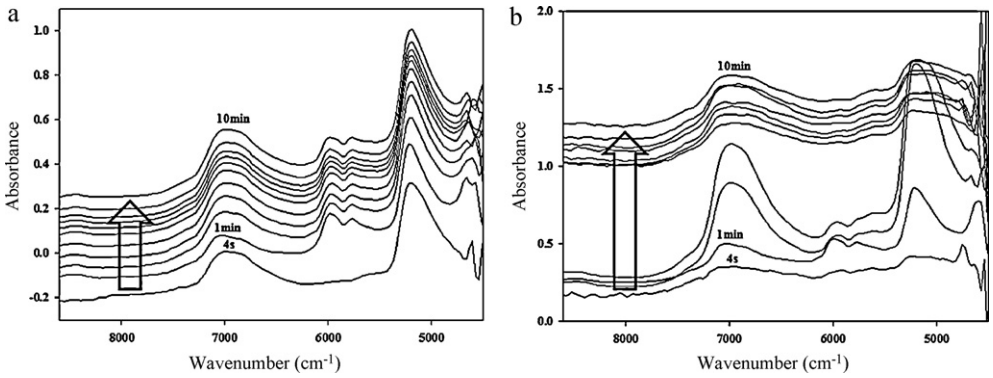

Fig. 3. NIR spectra acquired during IMC crystallization process (the first spectrum at 4 s and the rest 10 spectra at every minute from 1 to 10): (a) S-to-A scheme and (b) A-to-S scheme.

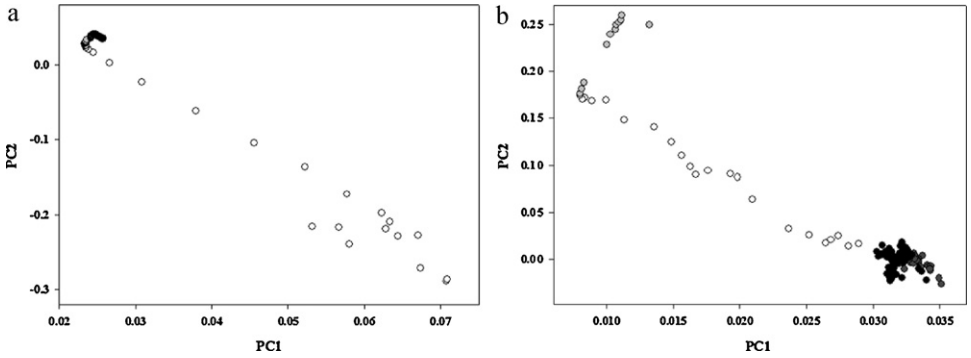

Fig. 4. PC score plots of IMC crystallization process: (a) S-to-A scheme and (b) A-to-S scheme.

during the whole crystallization process. Based on our preliminary analysis, NIR spectra from 4690 to 7500 cm^{-1} were chosen to perform qualitative and quantitative analyses. Fig. 3 compares the whole 10 min crystallization process for S-to-A (Fig. 3a) and A-to-S (Fig. 3b) schemes from a viewpoint of in-line NIRS. Each figure is composed of 11 NIR spectra, corresponding to every sampling minute of the process in addition to the first NIR spectrum acquired after 4 s. These two figures look apparently different. NIR spectra for the S-to-A scheme were gradually changing, whereas a rapid variation especially during its early stage (1–3 min), was detected for the A-to-S scheme.

A recent study reported that α-form IMC was readily produced by pouring an IMC-acetone solution into water as anti-solvent (Yokoyama et al., 1979). According to our experimental data, however, this S-to-A scheme gave a mixture of the γ-form and the α-form polymorphs. According to XRD analysis, the α-form fraction gradually increased to 71% as the crystallization was finished at 10 min. On the other hand, the A-to-S scheme surprisingly produced a highly pure α-form IMC powder as confirmed by its needle shape.

Typical PCA score plots of the S-to-A and A-to-S schemes are illustrated in Fig. 4. Each data point signifies a single NIR spectrum that was acquired at every 4 s. Again, these two look substantially different as mentioned in Fig. 3. For the S-to-A case, data points moved very quickly from the bottom right to the top left and then stayed there with a slight spatial variation as the crystallization process reached the end point. For the A-to-S scheme, on the other hand, plot points moved back to the initial area after a quick move from the bottom right to the top left, followed by a short trip toward the upper right. This observation exactly matches the results depicted in Fig. 3b as well.

The NIR spectra from 4 to 10 min looked like the one after the first 4 s. In addition, the data points of the PC score plot returned back to their initial location. It should be a very unusual coincidence, however, because they cannot be identical or similar to each other by any means. The NIR spectrum at 4 s is for a particle-free IMC solution, while the spectra at 4–10 min are for IMC solutions containing a substantial amount of IMC crystal particles.

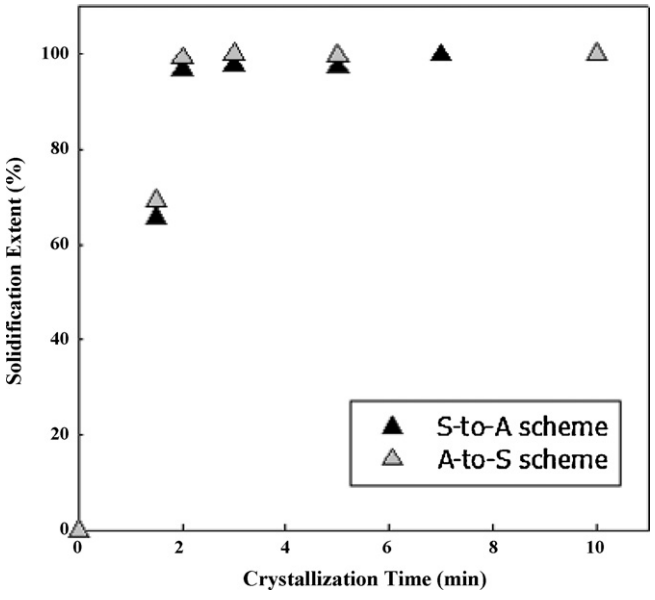

Fig. 5. Plot of solidification extent versus crystallization time.

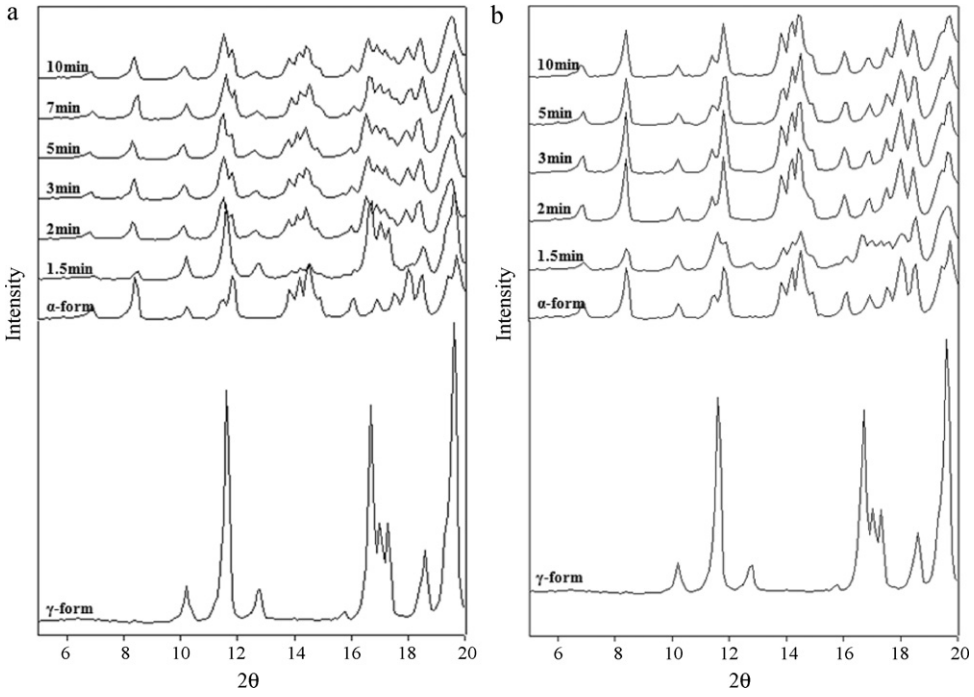

Fig. 6. XRD patterns of samples during IMC crystallization process: (a) S-to-A scheme and (b) A-to-S scheme.

3.2. Off-line characterization

Fig. 5 shows a plot of solidification extent versus process time. The extent value was calculated as the percentage of the powder solidified with respect to the total amount of IMC. No appreciable increase in powder weight was observed after 2 min for either scheme. For the off-line characterizations by XRD, SEM, and DSC, solution samples of 30 mL each were taken at 0.5 min, 1 min, 1.5 min, 2 min, 3 min, 5 min, 7 min, and, finally, at 10 min. Powder samples corresponding to shorter times such as 0.5 min and 1 min, however, were not obtainable due to serious difficulties in filtration. Filter papers were instantaneously clogged when the sampled IMC solutions underwent filtration. This clogging problem seems to be attributed to very fine particles that were created either during the crystallization or during the filtration itself.

Fig. 6 illustrates XRD pattern changes for S-to-A and A-to-S schemes compared with pure γ-form and α-form powders. For the S-to-A case, the XRD pattern at 1.5 min shows that the produced IMC powder was a mixture of the γ-form and the α-form. As the crystallization process continued, the intensity of the γ-form decreased while that of the α-form increased. Considering the peak at 12.6°, the final product should be a mixture of two polymorphs. As for the A-to-S scheme, the spectrum at 1.5 min signifies that the powder created was also a mixture of the γ-form and the α-form. After 2 min, the γ-form completely disappeared to give pure powder of the α-form. Since then, there was no noticeable change in the XRD pattern with respect to processing time.

For a quantitative analysis, areas under the diffraction peak regions 12.2–12.9° and 7.6–8.9° were computed via integration for the γ-form and the α-form, respectively. These area values were converted to approximate fractions of the γ-form, α-form, or amorphous phase based on the previous calibration equations. Since the Scherer method for the estimation of crystallite size correlated with broadening extent did not work out significantly, the size estimation of IMC powders was based on SEM and optical microscopy. These results are all put together for a comprehensive discussion in the following section.

Table 1
Measured solubility of IMC in acetone-water mixture of various compositions.

	Acetone fraction (%)						
	0.0	16.7	30.0	50.0	70.0	83.3	100
Solubility (mg/mL)							
γ-form	0.07	0.12	0.14	5.00	169.8	216.5	279.1
α-form	0.04	0.06	0.11	4.97	193.7	232.6	321.1

3.3. Solubility of the γ-form and α-form in mixture solvents

Table 1 summarizes the measured solubility of the γ-form and α-form in the acetone-water mixture of various fractions at 54 °C. The γ-form showed an appreciably greater solubility than the α-form in a water-rich solvent, which signifies that the stable form under this circumstance should be the α-form. When an acetone-rich solvent was used for salvation, the reverse is true. It seems interesting to observe the solubility of both polymorphs was changing abruptly in the 40–60% fraction range. The acetone fraction selected in this anti-solvent crystallization study was 16.7%. Hence, we can expect to obtain the α-form preferentially over the γ-form under normal conditions.

3.4. Stepwise interpretation of the S-to-A and A-to-S schemes

Figs. 7 and 8 summarize integrated PC score plots for the anti-solvent crystallization combined with the XRD and microscopy results under the S-to-A and the A-to-S schemes, respectively. All dots were illustrated in four different color tones in the following chronological order: white → light gray → dark gray → black. The final point corresponds to the completion point at 10 min. The region of primary interest in Fig. 4a was enlarged as enclosed with an ellipse in Fig. 7.

For the S-to-A scheme, dots are divided into three groups, which would indicate that the whole crystallization process is composed of at least three distinct steps. In terms of process time, the first step took place in the first 1.5 min. IMC particles at 1.5 min were mostly

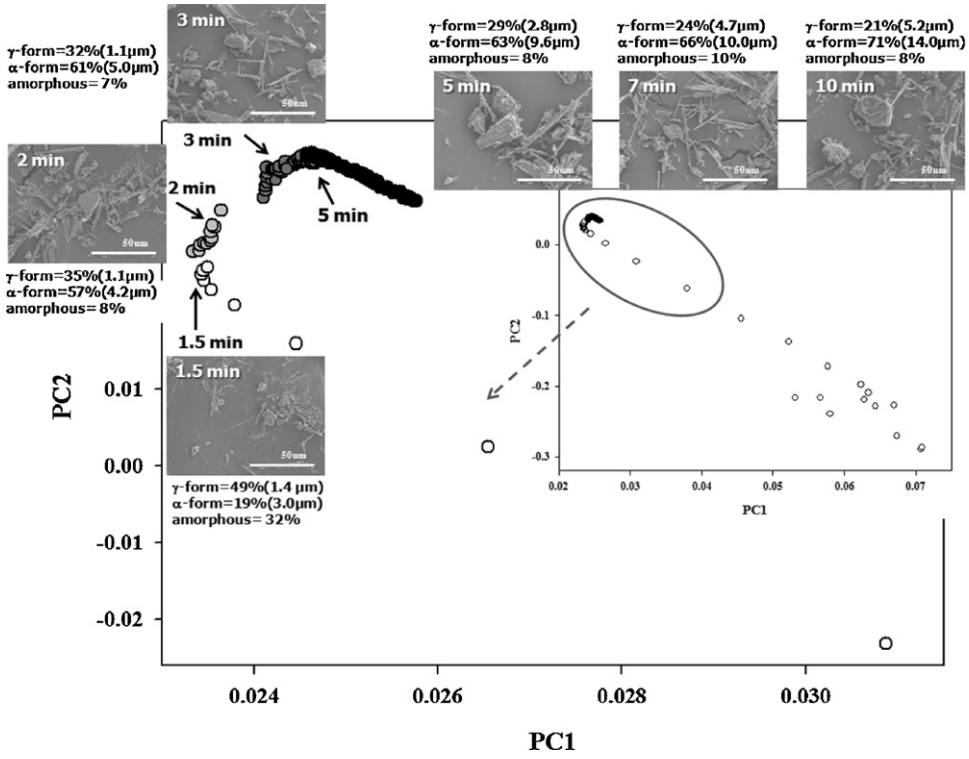

Fig. 7. An overall diagram for IMC anti-solvent crystallization process under S-to-A scheme.

γ-form (49%) and amorphous (33%) entities with a lesser amount of the α-form (19%). During the second step, from 1.5 min to 4 min, the α-form fraction increased greatly to 60% at the expense of the amorphous form, whereas the γ-form content decreased slightly to 30%. In this stage, however, increases in particle sizes were not remarkable. The third step, from 4 to 10 min, was distinguished by changes not in polymorphic fractions, but in particle size. Therefore, the crystallization under an S-to-A scheme can be represented as the nucleation of IMC particles into three distinctive polymorphs (γ-form, α-form, amorphous) followed by the polymorphic transformation primarily from the amorphous to α-form. Crystallization for 10 min was completed with substantial crystal growth by the final step.

The A-to-S scheme, as shown in Fig. 8 can be interpreted in an even simpler way. This case also can be divided into three steps. The first step, in the first 1.5 min, is the nucleation of IMC, this time mostly into the α-form (60%) and the γ-form (33%) with a minority of amorphous (7%) phase. In a way, this composition looks very similar to that at 2 min in Fig. 7. Subsequently, all other polymorphs other than the α-form completely disappeared at 2 min. The final step is actually not a usual change mechanism, but rather an instantaneous jump. As shown in Fig. 8, all dark-gray dots and black dots were gathered to a certain narrow region on the bottom right of the PC score plot. This result was very reproducible. There was no noticeable difference between off-line characterization data of IMC powders sampled at 3, 5, 10 min with respect to the polymorphic composition, solid weight gain, or particle size. Therefore, this pathway appears to be completed right after 2 min.

The two distinctive behaviors of the anti-solvent crystallization depending on the mixing scheme of the solution and

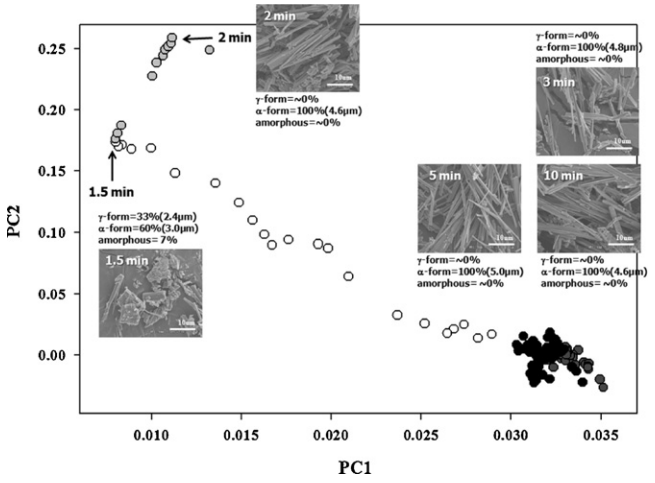

Fig. 8. An overall diagram for IMC anti-solvent crystallization process under A-to-S scheme.

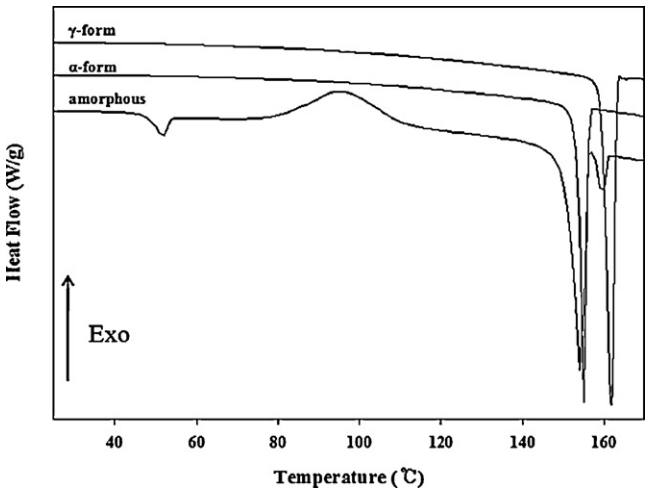

Fig. 9. DSC curve of standard IMC powders and amorphous.

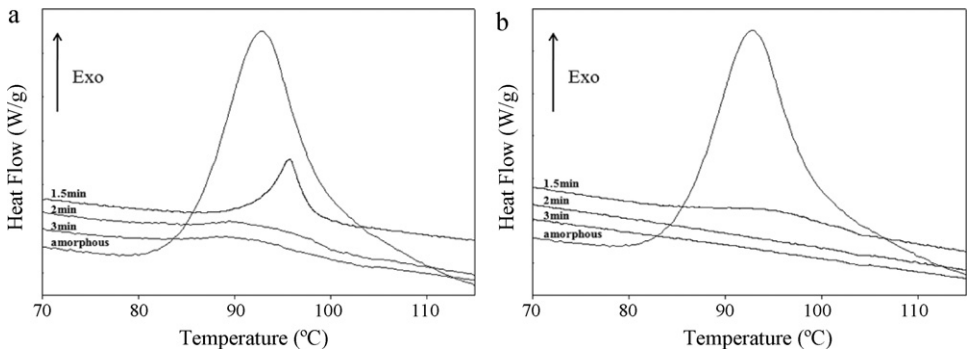

Fig. 10. DSC curve of samples during IMC crystallization process: (a) S-to-A scheme and (b) A-to-S scheme.

anti-solvent are explained in terms of the initial supersaturation and solution/anti-solvent composition. According to Ostwald's rule of stage, the high suspersaturation initiates preferentially the metastable crystals and then they are transformed to the stable one. Thereby, in the S-to-A scheme, the contact of the acetone-IMC solution to the water anti-solvent may induce the locally high supersaturation in the water-rich phase, which is favorable for the metastable nucleation of γ- and amorphous forms. Thus, at the early stage of the crystallization (1.5 min), the solid product appears mostly composed of the mastastable γ- and amorphous forms.

In contrast, the A-to-S scheme may instantaneously create the acetone-rich phase locally by the initial contact of the water anti-solvent to the acetone-IMC solution, in which the α-form is metastable and preferentially nucleated, as expected from the solubility data in Table 1. After then, the solution is homogenously mixed with the anti-solvent, varying finally to the water-rich phase as the bulk volume ratio of the solution to anti-solvent. At this stage, the γ-form becoming metastable is dominantly nucleated. Due to the simultaneous growth of the α-form initially nucleated, however, the nucleation of the γ-form would be limited. Thus, its fraction in the solid product is much lower than that at the same crystallization time (1.5 min) in the S-to-A scheme. It should be mentioned that the initial acetone-rich phase induced instantaneously in the A-to-S scheme would also be favorable for the generation of amorphous form. However, due to its high solubility in the acetone-rich phase, the supersaturation would not be so high enough to induce the amorphous solids as much as the water-rich phase in the S-to-A scheme.

Such explanation to the crystallization behaviors depending on two mixing scheme of the solution and anti-solvent is simply supported by the supplementary experiments varying the solution feeding rate. In this experiment, the acetone-IMC solution of 100 mL is slowly fed during certain time periods of 1 min, 3 min, 5 min and 10 min, instead of instantaneous pouring into the anti-solvent. This controlled feeding results in the definite reduction of the metastable form fraction at the end of the crystallization because the slow feeding rate induces the low initial supersaturation level which is less favorable for the nucleation of metastable forms and correspondingly more for the nucleation of stable form. Thus, as increasing the feeding time (slow feeding rate), the metastable form fraction at the end of fraction is lowered and completely disappeared at above 3 min of the feeding time.

Of the three polymorphic mixtures in the crystallization, the less stable γ-form is spontaneously transformed to the stable α-form via the solvent-mediated phase transformation process. Also, the least stable amorphous form would be changed to the α-form through γ-form. Thus, the fractions of the γ- and amorphous forms are continuously reduced and the fraction of the α-form increase correspondingly along with the crystallization time. Here, the transformation process is enhanced as increasing the initial fraction of stable form because it provides the larger surface area for the mass transfer in this process. Thus, the phase transformation in the A-to-S scheme appears much faster than in the S-to-A scheme, resulting in the complete conversion of the γ- and amorphous forms to the a-form within 2 min. It can be confirmed by the greater initial fraction of the α-form in the A-to-S scheme than in the S-to-A scheme, and is also consistent with the supplementary experiment above.

Fig. 9 illustrates three DSC curves of the synthesized amorphous IMC powder in addition to the standard γ-form and α-form powders. Two standard IMC powders showed their own endothermic peaks at 155 °C (α-form) and 162 °C (γ-form), respectively. On the other hand, the synthetic amorphous powder presented a glass transition temperature (T_g) at around 50 °C, whose reported value is 47 °C (Liu, 2008). The exothermic transition observed near 95 °C should be associated with the crystallization of amorphous IMC because an approximate prediction of the crystallization temperature gave 102.5 °C by the following expression (Liu, 2008).

$$T_c \doteqdot T_g + \frac{T_m - T_g}{2}$$

Since two separate endothermic peaks at ~153 °C and later at ~160 °C were observed and since no apparent exothermic peak was detected between these two temperatures, it appears that the amorphous IMC turned to two polymorphs, but mostly to the α-form during the crystallization which took place at 80–110 °C region.

Fig. 10 compares the detailed shape of DSC curves for polymorphic transformation at around 95 °C. As shown in Fig. 10a for an S-to-A scheme, the profile at 1.5 min shows a greater peak than those at 2 and 3 min, although their peak size was much smaller than that of the synthetic amorphous powder sample. In Fig. 7, the amorphous fraction at 1.5 min (33%) was greatly decreased to 8% at 2 and 3 min. Therefore, these two data seem to match for each other reasonably well.

Similar observations can be made in Fig. 10b for an A-to-S scheme as well. IMC powder at 1.5 min, whose amorphous fraction was 7% as in Fig. 8, showed a profile very close to the powders for 2 and 3 min, with an amorphous fraction of 8%, in Figs. 7 and 10a. On the other hand, the DSC curves of IMC samples at 2 and 3 min, that contain no amorphous phase material, do not show any comparable peaks. Therefore, the existence and transformation of the transient amorphous phase was presumed.

The most valuable advantage of a PCA application for in-line NIR measurements should be its capability for real-time monitoring during the whole crystallization process based on the spatial disposition of data points. Because PC score plots were obtained in a highly reproducible manner, some unexpected progress during the process should be instantaneously detected and handled with corrective measures that were prepared by control strategy.

4. Conclusions

We have monitored the anti-solvent crystallization process of indomethacin (IMC) under two schemes (S-to-A and A-to-S), employing in-line NIR spectroscopy. Based on off-line characterization results, those two schemes resulted in substantially different consequences. Highly pure α-form IMC was produced by the A-to-S approach, whereas a powder mixture of the γ-form and the α-form resulted from using the S-to-A scheme. Under an S-to-A scheme, the creation of γ-form was preferred due to a localized acetone-rich solvent condition, which resulted in a high initial γ-form fraction. The γ-form and the amorphous phase were transformed to the stable α-form eventually with particle growth. For the A-to-S circumstance, a similar phenomenon took place initially, but was followed this time by an extraordinary movement to create pure α-form particles.

Based on the PCA plots, each scheme can be divided into three steps. Each step was well elucidated in accordance with off-line XRD, DSC and microscopic off-line characterizations. In addition, PC score plots were very reproducible. Any noticeable deviation off the expected pathway in the PC score plot should be detected in real time. Therefore, it was demonstrated that PCA could be utilized for in-line monitoring of the solution crystallization process toward a PAT implementation in terms of polymorphism and particle size.

Acknowledgements

This study has been fully supported by the 2009 Inje University Research Promotion Grant. In addition, we acknowledge the instrumental assistance from ABB as well as for in-line NIR spectroscopy.

References

Beckmann, W., 1999. Nucleation phenomena during the crystallization and precipitation of Abecarnil. J. Cryst. Growth 199, 1307–1314.

Chen, X., Morris, K.R., Griesser, U.J., Byrn, S.R., Stowell, J.G., 2002. Reactivity differences of indomethacin solid forms with ammonia gas. J. Am. Chem. Soc. 124, 15012–15019.

Chieng, N., Aaltonen, J., Saville, D., Rades, T., 2009. Physical characterization and stability of amorphous indomethacin and ranitidine hydrochloride binary systems prepared by mechanical activation. Eur. J. Pharm. Biopharm. 71, 47–54.

Heinz, A., Savolainen, M., Rades, T., Strachan, C.J., 2007. Quantifying ternary mixtures of different solid-state forms of indomethacin by Raman and near-infrared spectroscopy. Eur. J. Pharm. Sci. 32, 182–192.

Holmback, X., Rasmuson, A.C., 1999. Size and morphology of benzoic acid crystals produced by drowning-out crystallization. J. Cryst. Growth 199, 780–788.

Kaneko, S., Yamagami, Y., Tochihara, H., Hirasawa, I., 2002. Effect of supersaturation on crystal size and number of crystals produced in antisolvent crystallization. J. Chem. Eng. Jpn. 35, 1219–1223.

Kaneniwa, N., Otsuka, M., Hayashi, T., 1985. Physicochemical characterization of indomethacin polymorphs and the transformation kinetics in ethanol. Chem. Pharm. Bull. 33, 3447–3455.

Kistenmacher, T.J., Marsh, R.E., 1972. Crystal and molecular structure of an antiinflammatory agent, indomethacin, 1-(p-chlorobenzoyl)-5-methoxy-2-methylindole-3-acetic acid. J. Am. Chem. Soc. 23, 1340–1345.

Kitamura, M., Sugimoto, M., 2003. Anti-solvent crystallization and transformation of thiazole-derivative polymorphs—I: effect of addition rate and initial concentrations. J. Cryst. Growth 257, 177–184.

Liu, R. (Ed.), 2008. Water-Insoluble Drug Formulation. CRC Press, pp. 531–561.

Masuda, K., Tabata, S., Kono, H., Sakata, Y., Hayase, T., Yonemochi, E., Terada, K., 2006. Solid-state ^{13}C NMR study of indomethacin polymorphism. Int. J. Pharm. 318, 146–153.

O'Grady, D., Barrett, M., Casey, E., Glennon, B., 2007. The effect of mixing on the metastable zone width and nucleation kinetics in the anti-solvent crystallization of benzoic acid. Chem. Eng. Res. Des. 85, 945–952.

Oosterhof, H., Witkamp, G.J., van Rosmalen, G.M., 1999. Some anti-solvents for crystallization of sodium carbonate. Fluid Phase Equilibr. 155, 219–227.

Otsuka, M., Kato, F., Matsuda, Y., Ozaki, Y., 2003. Comparative determination of polymorphs of indomethacin in powders and tablets by chemometrical near-infrared spectroscopy and x-ray powder diffractometry. AAPS PharmSciTech 4 (2), 1–12.

Slavin, P.A., Sheen, D.B., Shepherd, E.E.A., Sherwood, J.N., Feeder, N., Docherty, R., Milojevic, S., 2002. Morphological evaluation of the g-polymorph of indomethacin. J. Cryst. Growth 237–239, 300–305.

Takiyama, H., Otsuhata, T., Matsuoka, M., 1998. Morphology of NaCl crystals in drowning-out precipitation operation. Chem. Eng. Res. Des. 76, 809–814.

Takiyama, H., Minamisono, T., Osada, Y., Matsuoka, M., 2010. Operation design for controlling polymorphism in the anti-solvent crystallization by using ternary phase diagram. Chem. Eng. Res. Des. 88, 1242–1247.

Urakami, K., Shono, Y., Higashi, A., Umemoto, K., Godo, M., 2002. A novel method for estimation of transition temperature for polymorphic pairs in pharmaceuticals using heat of solution and solubility data. Chem. Pharm. Bull. 50 (2), 263–267.

US-DHHS, US-FDA, 2002. Pharmaceutical CGMPs for the 21st century: a risk-based approach; a science and risk-based approach to product quality regulation incorporating an integrated quality systems approach, http://www.fda.gov/oc/guidance/gmp.html.

US-DHHS, US-FDA, 2004. CDER/CVM/ORAPAT—a framework for innovative pharmaceutical development, manufacturing, and quality assurance, Pharmaceutical CGMPs.

Winter, C.A., Risley, E.A., Nuss, G.W., 1963. Anti-inflammatory and antipyretic activities of indomethacin, 1-(p-chlorobenzoyl)-5-methoxy-2-methyl-indole-3 acetic acid. J. Pharmacol. Exp. Ther. 141, 369–376.

Yokoyama, T., Umeda, T., Kuroda, K., Nagafuku, T., Yamamoto, T., Asada, S., 1979. Studies on drug non-equivalence IX: relationship between polymorphism and rectal absorption of indomethacin. Yakugaku Zasshi 99, 837–842.

Yu, Z.Q., Tan, R.B.H., Chow, P.S., 2005. Effects of operating conditions on agglomeration and habit of paracetamol crystals in anti-solvent crystallization. J. Cryst. Growth 279, 477–487.